AN IMPLICIT GEOMETRIC REGULARIZATION OF 3D BUILDING SHAPE USING AIRBORNE LIDAR DATA

Y. Jwa[a], G. Sohn[a] , V. Tao[a], W. Cho[b]

[a]GeoICT Lab, York University, 4700 Keele St., Toronto, ON M3J 1P3, Canada –(yjwa, gsohn, tao)@yorku.ca
[b]Dept. of Civil Engineering, Inha University, 253 Yonghyun-dong Nam-gu, Incheon, South KOREA - wcho@inha.ac.kr

Commission III, WG III/3

KEY WORDS: LIDAR, Building, Edge, Incremental, Generalization, Reconstruction

ABSTRACT:

The prime objective of this paper is to develop a new method for regularizing noisy building outlines extracted from airborne LiDAR data. For the last few decades, a lot of research efforts have been made towards the automation of building outline regularization, which include Douglas-Peucker's polyline simplication, least-square adjustment, model hypothesis-verification, and rule-based rectification. This paper presents a new method to rectify noisy building polylines by dynamically re-arranging quantized line slopes in a local shape configuration and globally selecting optimal outlines based on the Minimum Description Length principles. The optimality is achieved when a building polyline is maximally hypothesized as the repetition of identical line slope and inner angular transition are enhanced with minimal numbers of vertices. A comparative evaluation of the proposed regularization method is compared with existing methods using simulated building vectors with different random errors. The results show that the proposed method outperforms the selected existing algorithms at the most of noise levels.

1. INTRODUCTION

3D building geometric modelling in urban areas is in great demand for a variety of applications such as urban planning, mobile communication, 3D city modelling and virtual reality (Sohn and Dowman, 2007). Since human-centric building modelling is time consuming and very costly, a fast and general method for simplifying irregular building boundary lines based on segmentation results is highly required in dynamically changing urban areas. In the last few decades, considerable research effort has been directed toward mainly reconstructing building models using aerial imagery and airborne laser scanning data obtained from passive and active sensors such as camera and laser scanner (Weidner et al., 1995; Ameri, 2000; Sohn and Dowman, 2007; Sohn et al., 2007; Sampath et al., 2007). However, the current state-of-the-art techniques in 3D building reconstruction have not been matured yet, and still produce large errors in reconstructed building outlines. Thus, many enthusiastic researchers have introduced different techniques in the geometric regularization. However, these research efforts have gained only limited success in constrained environments requiring many pre-specified thresholds to control the geometric regularity which are not often the case in practice. Therefore, developing the new technique to implicitly drive regularization rules from given data domain is urgently required.

This study is organized into six sections. Section 2 discusses the existing regularization methods selected for current comparative performance test. In Section 3, we introduce a new geometric regulator developed based on Minimum Description Length (MDL). Section 4 presents a comparative analysis of the proposed technique's performance with the selected geometric regulators. Quality assessment for each method is provided using the geometric regularity error matrix in Section 5. Finally the paper will end with some concluding remarks and recommendations for future research.

2. PREVIOUS RESEARCH WORKS

For the last few decades, many research works concerning the geometric regularization of 3D building shape has been conducted. We selected four representative techniques from the literature to conduct a comparative analysis of the geometric regularization over noisy building vectors. Theses include Douglas-Peucker's algorithm (Douglas and Peucker, 1973), Local Minimum Description Length (Weidner and Förstner, 1995), Feature Based Model Verification (Ameri, 2000) and Rule-based Rectification (Sampath and Shan, 2007). In this section, we briefly explain the above listed algorithms, which performance will be later compared to a new regularization method proposed in this study.

2.1 Iterative Polyline Simplication

The classical Douglas-Peucker (DP) line-simplication algorithm has been widely recognized as the most visually effective line simplication algorithm (Ramer, 1972). This simple algorithm start to construct a polyline with edge segments which link *a prior* initial vertex selected from edge points. The process recursively discards the subsequent vertices whose distance from the initial polyline less than $\zeta > 0$ error tolerance, but accepts the vertex as part of the new simplified polyline if it is farther away from the line larger than ζ, which becomes the new initial vertex for further simplication. This process continues until all remaining vertices from the initial polyline are less than ζ.

2.2 Model Hypothesis-Verification

Weidner and Förstner (1995) regularized nosy building outlines extracted from high-resolution DSM using MATCH-T based on a local Minimum Description Length (LMDL). The MDL principal is well-known optimization method to find a good balance between nominal error distribution and model complexity based on Occam's razor. Starting from the initial building boundary obtained from the DP algorithm, the method select four consecutive points as a local unit of the polyline regularization. With this local point set, the ten different hypothetical regularization models are generated (Figure 1). The hypotheses are generated to consider the orthogonality between consecutive lines by moving two middle points or to enhance the simplicity by removing one of the middles points.

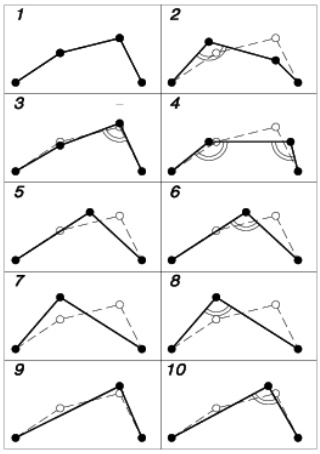

Figure 1. Ten alternative hypotheses for local configuration with optimum case 10 (Weidner et. al., 1995).

For each hypothesis, the description length, *DL*, is measured on the goodness-of-fit between the hypothesized model and its corresponding observations and on the model complexity. Given a regularization hypothesis, *H*, and the observation, *D*, *DL* is now defined as

$$DL = L(D|H) + L(H) \tag{1}$$

where $L(D|H)$ is the likelihood of *H* describing *D* and $L(H)$ is the complexity measure of *H*. Weidner and Förstner (1995) suggested $L(D|H)$ and $L(H)$ in Eq. (1) as

$$DL = -\frac{\Omega}{2} ln\, 2 + \frac{\left(N_p - N_c\right)}{2} lb\, N_p \tag{2}$$

In Eq. (2), Ω is the weight sum of the squared residuals between *D* and *H*. *H*'s complexity in the last term of Eq. (2) depends on the number of unknown parameter, N_p (i.e., the number of vertices associated to generate *H*), and constraints, N_c (i.e., the number of parameters to constrain the orthogonality. The optimal hypothesis, H^*, is determined by simultaneously minimizing Ω and the number of vertices used to generate *H*.

Because of local-based approach, this method can produce different results according to starting point among building boundary points when regularization process is performed. That is, the shape of regularized polygon can be changed according to the starting point of the procedure. In order to achieve the global geometric relation of resulting polygon, another global hypothesis such as orthogonality and parallelity is needed.

2.3 Least-Squares′ Adjustment

Ameri (2000) introduced the Feature Based Model Verification (FBMV) for regularizing 3D polyhedral building shape extracted from high-resolution multiple airborne images. The method is developed based on the total least-squared adjustment. In here, the approach is implemented by using only laser scanning data. The first step of FBMV is to extract initial value for vertices and line parameters by DP algorithm. Then, these edge points serve to compute building planar parameters. Finally, the total least-squared adjustment is performed based on linearity, connectivity, coplanarity, and orthogonality as shown in Eq. 3. The linearity constraint is used to minimize the perpendicular distance between LiDAR data and representative lines per each segment. The intersection coordinate of two adjacent lines can be computed based on the connectivity constraint. The coplanarity constraint is applied under the assumption that all boundary points must be located on the same planar surface. Since the constraints in Eq.3 are formed as nonlinear equation, the equations must be used after changing them to linearized forms.

$$\begin{aligned}
&L(\theta_j,\rho_j) = x_i\cos\theta_j + y_i\sin\theta_j - \rho_j \qquad \underline{e} \sim N\left(\underline{0},\ \sigma_0^2 P_L^{-1}\right)\\
&C(\theta_j,\rho_j,x_j^I,y_j^I) = x_j^I\cos\theta_j + y_j^I\sin\theta_j - \rho_j \quad \underline{e} \sim N\left(\underline{0},\ \sigma_0^2 P_C^{-1}\right)\\
&P(x_j^I,y_j^I,z_j^I) = ax_j^I + by_j^I + c - z_j^I \quad \underline{e} \sim N\left(\underline{0},\ \sigma_0^2 P_P^{-1}\right)\\
&O(x_j^I,y_j^I,z_j^I) = a_1a_2 + b_1b_2 + c_1c_2 \quad \underline{e} \sim N\left(\underline{0},\ \sigma_0^2 P_O^{-1}\right)
\end{aligned} \tag{3}$$

x_i, y_i, z_i : 3D coordinates from LiDAR data

θ_j, ρ_j :Angle between edge and x axis,
distance between origin and line

x_j^I, y_j^I, z_j^I : 3D coordinate of intersections between edges

a, b, c : Plane components

$a_{1or2}, b_{1or2}, c_{1or2}$: Direction vectors for two edges

L, C, P, O : Linearity, Connectivity, Coplanarity, Orthogonality

In case of orthogonality, if α (angle between vectors) exists within $t > 0$ the acceptable tolerance, the orthogonal property is applied to the vertex as

$$90^0 - t \le \alpha \le 90^0 + t \tag{4}$$

FBMV provides flexibility to control conditional constraints such as orthogonality, parallelity and symmetricity simultaneously. However, it still requires hard-constraints to facilitate these regulators. Similarly to the well-known least-square problems, the performance of FBMV is subject to initial conditions provided by DP.

2.4 Rule-based Rectification

Sampath & Shan (2007) developed a Rule-based Regularization (RR) for refining a coarse building boundaries extracted by classical supervised classification using IKONOS imagery. The method consists of two-step regularization processes. A coarse building boundary is obtained by DP, thereby eliminating noisy

boundary points. The second step is to further rectifying outlying points with perpendicular constraints which is pre-specified. After dividing slopes into two groups in horizontal and vertical direction, a simple least square adjustment is performed to regularize boundary lines with irregular shape. Since the slope direction is only divided into two directions, in case of the building polygon with more than two directions, the proposed regularizing process is not working well. However, this approach can rapidly provide the good solution for regularization in the building with simple shape. The line equation and orthogonal constraint equation can be used as shown in the following equation.

$$L(A_i, B_i) = A_i x_j + B_i y_j + 1 \quad \underline{e} \sim N\left(\underline{0}, \ \sigma_0^2 P_L^{-1}\right)$$
$$O(A_i, B_i, M_s) = \frac{A_i}{B_i} + M_s \quad \underline{e} \sim N\left(\underline{0}, \ \sigma_0^2 P_O^{-1}\right) \qquad (5)$$

x_j, y_j : Horizontal coordinates from LiDAR data

M_s : Slop for vertical or horizontal (=-1/ $M_{h,or,v}$)

L, O : Linearity, Orthogonal constraint ($M_h M_v = -1$)

3. A NEW BUILDING SHAPE REGULARIZATION

In this section, we propose a novel method for incrementally regularizing noisy building outlines by considering newly driven geometric regularity parameters in MDL framework. The optimal shape regularity is achieved by testing hypothetically regularized models with regularity favoured objective function.

3.1 LMDL Limitations

As shown in Weidner and Förstner (1995), the most benefit taken from the MDL regulator is that the method is generic not to require hard-constraints (i.e., pre-specified thresholds) to explicitly constrain the domain knowledge on the shape regularity. For instance, both FBMV and RR pre-specify an if-then rule set to facilitate the regulator following the orthogonality and parallelity, which is only working well with certain limited condition. However, the MDL provides more flexibility to implement such regularization rules with soft-constraints (i.e., cost function or objective function).

In LMDL, the cost function is to minimize the description lengths which bitwise encode the cost to select a hypothetical model when it is true in terms of the residual likelihood and the model complexity. The optimization of LMDL is achieved by verifying entire model candidates that are generated with different model complexity. An optimized model will be achieved to produce reasonable residuals with the simplest model. Although LMDL was successfully applied to the building shape regularization problem, we have observed two major limitations that could be improved; (1) locality and (2) limited encoding scheme for the model complexity. LMDL is conduced over a local set of four consecutive points, by which: firstly, the regularization result by LMDL depends on starting local point set and secondly, the orthogonality and parallelity to generate hypothetical models are relatively determined in relation to the positions of the two (starting and ending) anchor points of the local point set. Moreover, the model complexity is only penalized by the number of the vertices forming the model. However, with the same number of vertices, polygons with different model complexity can be made.

3.2 Geometric MDL

We propose a new method to regularize noisy building outlines, called Geometric MDL (GMDL), which encodes the model complexity with different regularity measurements from LMDL. In GMDL, we define the shape regularity to show: (1) the directional repeatability, (2) the regular angle transition, and (3) the number of model parameters. That is, the optimal model is selected if the polyline has as many as possible identical line directions, N_D; smoother or more orthogonal inner angle transition between adjacent lines, $Q_{\Delta\theta}$; and smaller numbers of vertices, N_P. This can be described in MDL framework as

$$DL(H) = -\frac{\Omega}{2} ln\, 2 + W_D N_D \log_2 N_P + W_{\Delta\theta} Q_{\Delta\theta} \log_2 N_P + W_P K \log_2 N_P \qquad (6)$$

In Eq. (6), the first term describes the closeness between model and observation as in Eq. (2), and the last term indicates the model complexity. Note that the weight factors (W_D, W_P, $W_{\Delta\theta}$) are firstly settled as default value such as one. Ω is the sum of the squared residuals between model and observation.

3.3 Methodology

An optimization strategy to determine H^* that minimises Eq. (6) is comprised of following tasks.

3.3.1 *Initial Vectorization*: After ordering building boundary points by using a modified convex-hull method, an initial building outlines are reconstructed with linked edge segments obtained by DP algorithm.

3.3.2 *Quantizing Line Directions*: We apply Compass Line Filter (CLF) developed by Sohn et al. (2007) to initial line segment, which is quantized into one of eight line directions. CLF is designed as a set of quantized line direction $\{\theta_i: i=1,\ldots,8\}$, where the direction of the first compass line is horizontal and the others are spaced with equally 22.5 degree as shown in Figure 2.

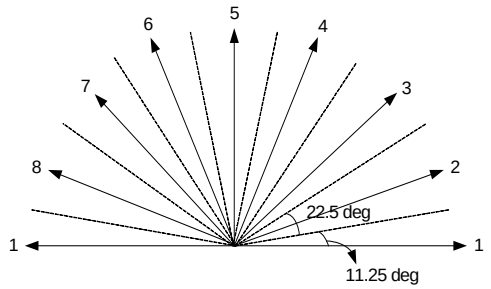

Figure 2. Illustration of CLF: A set of quantized line directions with 22.5°

All line directions $\{\theta\}$ are measured by $xsin\theta - ycos\theta = d$ and assigned into one of eight CLF numbers, where θ indicates the angle between a line segment and *x-axis*, and d is the line distance from the origin. Finally, the representative line directions with respect to each CLF number are calculated by weight-averaging cumulative directions belonging to the same CLF number.

3.3.3 *Computing Model Complexity*: Once all the lines are grouped with respect to CLF, the total numbers of line directionality (N_D), which are ranged between one and eight, forming building outlines are determined. The angular transitional regularity ($Q_{\Delta\theta}$) are determined to have the minimum score of 0 (i.e., favoured regularity) if the inner angle difference between two consecutive lines close to 90˚ or 180˚, while the maximum score of 2 (i.e., un-favoured regularity) as in general the building outlines with the acute angle at one vertex is rare, the penalty value must be assigned with higher value compared to the other index numbers (Table 1).

i	$\Delta\theta i$	$Q_{\Delta\theta i}$
1	0.0 ~ 11.25	2
2	11.25 ~ 33.75	1
3	33.75 ~ 56.25	1
4	56.25 ~ 78.75	1
5	78.75 ~ 101.25	0
6	101.25 ~ 123.75	1
7	123.75 ~ 146.25	1
8	146.25 ~ 168.75	1
9	168.75 ~ 180.00	0

Table 1. Quantized $Q_{\Delta\theta}$.

3.3.4 *Regularizing Hypothesis Generation*: For each vertex, GMDL generate a number of regularizing model hypothesis in two different ways. Instead of selecting the four local point set used in LMDL, GMDL selects three vertices to generate hypothetical solutions (Figure 3): (1) the anchor point, v_1, that are fixed during the hypothesis generation; (2) the floating point, v_2, that could be movable; (3) the guiding point, v_3, that provides a guidance how v_2 moves.

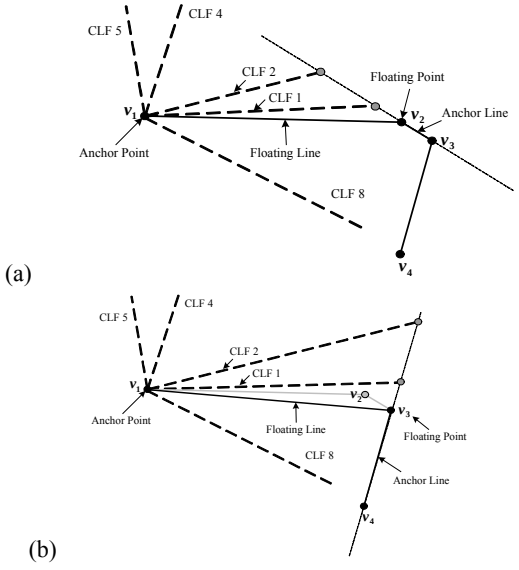

Figure 3. The possible alternative hypotheses at anchor point: (a) by moving v_2 and (b) by eliminating v_2.

As illustrated in Figures 3(a), a number of hypothetical models are generated by moving v_1. A floating line centered at v_1 can move along the anchor line passing through v_2 and v_3 by replacing the floating line's direction with CLF's ones. By intersecting the floating and anchor lines, a new vertex is computed for hypothesizing a regularized model. Figure 3(b) shows alternative hypothesizing method by eliminating v_2. Once v_2 is eliminated, the floating lines are generated by the same way illustrated in Figure 3(a) and then, the floating and guiding point are changed to v_3 and v_4. Finally, a new vertex will be computed by intersecting the newly computed floating and anchor lines.

3.3.5 *Global Optimization*: The following Figure 4 and Table 2 show an example of GMDL regularization.

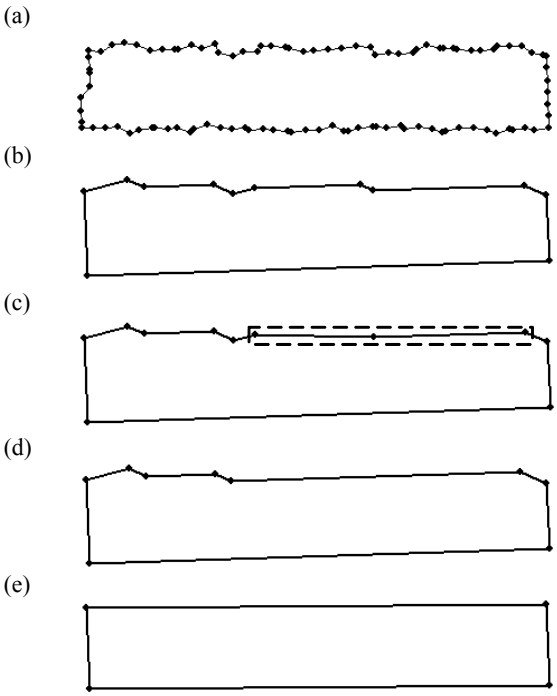

Figure 4. Principal steps of the regularization of irregular building boundary lines: (a) initial shape, (b) vectorization based on Douglas-Peucker approach, (c) reconstruction of lines within dotted line, (d)merge, (e) final optimal configuration

Figure 4(a) shows initial outlines formed by using boundary points extracted based on modified convex-hull algorithm after building detection. Figure 4(b) is the initial simplified polygon simplified by DP and initial DL value for the null hypothesis is calculated. In the next step (c), after computing {DL} for the entire vertices, the optimal hypothesis to produce the minimum DL, which is smaller than the null hypothesis, is selected (see the dotted box in Figure 4(c)). In Table 2, the null hypothesis's DL (Figure 4(b)) is larger than the one in Figure 4(c) because the configuration eliminating one of vertices from building outlines mainly contributes to the optimal configuration. If neighbouring line's directionality has the same CLF value, a simple merging procedure is performed as shown in Figure 4(d). The last step (Figure 4(e)) presents the final optimal outlines after recursively conducting the processes illustrated in Figure 4(c) and (d) until the minimum DL obtained at the current iteration is larger than the one at the previous iteration.

Step	N_P	N_D	$Q_{\Delta\theta}$	$L(M)$	Ω /2ln2	DL
(b)	12	4	3.33	34.65	22.61	57.26
(c)	11	4	2.66	30.55	23.62	54.17

(d)	9	4	3.11	25.53	24.26	49.79
(e)	4	2	0.0	6.00	15.82	21.82

Table 2. The values of DL elements in each step

4. EXPERIMENTAL RESULT

The performance of the proposed shape regularization techniques was estimated based on simulated 3D building points. 3D reference building vectors were manually captured, with which LiDAR points were generated by intersecting LiDAR rays with digitized 3D building vectors. The reference points were simulated to have a point density of 11 points/ m^2.

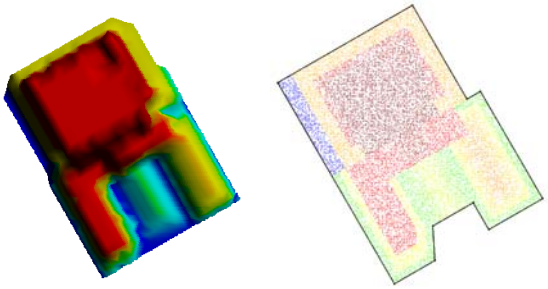

Figure 5. Simulated reference building points and boundary line in 3D (left) and 2D (right).

The reference building shown in Figure 5 was simulated with noise free condition that is all points were generated with about 0.3m point spacing. To evaluate different shape regularization methods under various noise levels in LiDAR data, we added the five random noises (±5cm, ±10cm, ±15cm, ±20cm and ±25cm) to the building boundary points extracted from reference. Note that these random errors are only considered in x-y horizontal directions because this study focuses on 2D shape reconstruction. The boundary points were extracted in a 2D buffer zone made around initial building outlines obtained by DP algorithm. The buffering size was heuristically determined based on the data domain knowledge of average point spacing for each test set. The first column of Figure 6 presents initial boundary lines extracted from the building test datasets simulated with five different noise scales. Based on these datasets, we applied the shape regularization methods (DP, LMDL, FBMV, RR, GMDL) that were discussed in previous sections. From the second to the sixth column in Figure 6 shows the results of regularization from initial boundary lines by the four regularization methods. All the algorithms were implemented using Microsoft Visual C++ and tested in the desktop computer with Intel's Pentium IV CPU with 1GB system memory.

5. QUALITY ASSESSMENT

In order to achieve optimal model selection in building boundary modelling, performance and cost factors of each model must be taken into account. Therefore, before selecting the optimal model to a building shape, the performance of each regularization model must be tested with respect to various factors. The quality of each reconstructed model is evaluated based on error matrix shown in Table 3. In Table 3, *R*, *E*, *P* and *V* refer to Reference, Extracted, Polygon and Vertex. The score, which is used to judge the suitability of each model, is calculated by summing each element of error matrix. The value closer to zero indicates to have higher shape regularization.

Category	Description
Vertex Complexity (VC)	$= \sqrt{\left(\frac{N_{RV} - N_{EV}}{N_{RV}}\right)^2}$ N : number of vertices
Angle Complexity (AC)	$= \frac{\sqrt{\Sigma(\delta\theta_{RP})^2} - \sqrt{\Sigma(\delta\theta_{EP})^2}}{\sqrt{\Sigma(\delta\theta_{RP})^2}}$ $\delta\theta$: difference between inner angles
Corner Difference (CD)	$= \sqrt{\Sigma(V_{RV} - V_{EV})^2}$ V : position of vertex
Orientation Difference (OD)	$= \sqrt{\Sigma(S_{RP} - S_{EP})^2}$ S : slop of main direction
CM Difference (CMD)	$= \sqrt{\Sigma(CM_{RP} - CM_{EP})^2}$ CM : center of mass
Area Difference (AD)	$= \sqrt{\left(\frac{A_{RP} - A_{EP}}{A_{RP}}\right)^2}$ A : Area

Table 3. Error matrix

Table 4 shows error measurements across tested regularization methods according to different noise levels from ±5cm to horizontal ±25cm horizontal random errors. As shown in Table 4, LMDL has a tendency to over-simplify building boundaries as shown in Figure 6(b) and (d). CD score for LMDL is more or less larger than the others because the slope directionality is decided based on local alternative models and constraints. FBMV's score significantly increases as the random noise level becomes higher. This is because FBMV does not consider achieving the model simplicity by eliminating noisy vertices. Thus, the induced errors become very high in VC and AC. In this context, we can conclude that FBMV is not suitable for regularizing building outlines corrupted with high noise level. In case of RR, the score shows better performance at the low noise level, but was rapidly lowered as the noise level becomes higher as pre-fixed simple rules cannot efficiently handle very noisy boundaries. As shown in Figure 6 and Table 4, the performance of GMDL is outstanding regardless of the complexity of building polygon.

Category		Error (cm)				
		±5	±10	±15	±20	±25
Vertex Complexity (VC)	LMDL	0.20	0.40	0.20	0.40	0.20
	FBMV	0.20	0.30	0.40	1.00	2.00
	RR	0.00	0.00	0.20	0.60	1.00
	GMDL	0.00	0.00	0.00	0.00	0.00
Angle Complexit	LMDL	0.08	0.06	0.46	0.10	0.09
	FBMV	1.98	3.00	4.41	8.19	21.0

y (AC)	RR	0.16	0.28	2.48	4.22	6.99
	GMDL	0.23	0.17	0.19	0.04	0.88
Corner Difference (CD)	LMDL	2.41	2.61	4.76	3.43	6.80
	FBMV	2.82	2.55	2.24	2.12	2.32
	RR	1.86	2.24	2.87	3.02	3.41
	GMDL	1.94	1.80	2.37	1.79	3.44
Orientation Difference (OD)	LMDL	0.32	0.16	0.36	0.15	0.29
	FBMV	0.3	0.42	0.57	0.53	0.21
	RR	0.01	0.01	0.32	0.21	0.82
	GMDL	0.01	0.02	0.00	0.00	0.08
CM Difference (CMD)	LMDL	0.25	0.13	0.55	0.15	0.28
	FBMV	0.23	0.22	0.20	0.10	0.03
	RR	0.04	0.04	0.06	0.05	0.03
	GMDL	0.05	0.06	0.07	0.07	0.03
Area Difference (AD)	LMDL	0.03	0.03	0.00	0.02	0.03
	FBMV	0.00	0.01	0.00	0.01	0.01
	RR	0.02	0.02	0.01	0.01	0.01
	GMDL	0.02	0.02	0.01	0.02	0.01
Total Score	LMDL	3.31	3.42	6.35	4.27	7.71
	FBMV	5.56	6.52	7.85	11.9	25.6
	RR	2.11	2.62	5.97	8.14	12.2
	GMDL	2.27	2.09	2.68	1.95	4.48

Table 4. Performance evaluation of tested geometric regulators according to different noise levels

6. CONCLUSIONS

This study presented the analysis of existing generalization methods and the new automatic regularization method of building irregular polygon, in which quantized line vectors are dynamically re-arranged based on MDL theory. The main aspect of proposed GMDL method is to provide a robust solution to incrementally regularize noisy building boundary by minimizing both residual errors and model complexity. A new objective function was introduced to augment geometric regularity in terms of the geometric repeatability, regular angle transition and the number of vertices used. We conducted a comparative evaluation of GMDL's performance with the four existing algorithms including DP, LMDL, FMBV and RR using simulated building data added with five different noise levels. The results showed that GMDL outperforms all the regulators selected at the most of noise levels, and GMDL's performance was measured approximately more than three times higher in average compared to the others at the highest noise level. Achieving the robustness against high noise level by GMDL is important for applying it to the real-setting environment. As future researches, we will extend GMDL from 2D vectors to 3D polyhedral cases, by which large-scale 3D building models can be incrementally refined in temporal domain.

ACKNOWLEDGEMENTS

This research was partly supported by a grant from Korean Land Spatialization Research Project funded by Ministry of Construction & Transportation of Korean government. The authors also like to appreciate the support of the project, "An Integrated Geomatics Project in Coastal Zone: Terrestrial, Airborne and Marine Data Fusion (FUDOTERAM)" – Project#SLMDFM-12, sponsored by GEOIDE Network Centres, Canada (http://www.geoide.ulaval.ca/home_EN.html).

REFERENCES

Ackermann, F., 1999. Airborne laser scanning-present status and future expectations, *ISPRS Journal of Photogrammetry and Remote Sensing*, 54(2), pp 64-67.

Ameri, B., 2000. Feature-Based Model Verification (FBMV): a new concept for hypothesis validation in building Reconstruction, In: *Proceedings of the XIXth ISPRS Congress, IAPRS, Vol. XIX, Part 3*, Amsterdam, the Netherlands, pp. 24-35.

Brunn, A., Weidner, U. and Förstner, W., 1995. Model-based 2D-Shape Recovery, In Sagerer, G., Posch, S., and Kummert, F., editors, *Mustererkennung*, 1995, pp. 260-268.

Douglas, D.H. and Peucker, T.K., 1973. Algorithms for the reduction of the number of points required to represent a digitized line or its caricature. *Canadian Cartographer*, 10(2):112-122.

Ramer, U., 1972. An iterative procedure for the polygonal approximation of plane curves. *Computer graphics and Image Processing*, 1:224-256.

Rissanen, J., 1984. Universal coding, information, prediction, and estimation. IEEE *Transaction of Information Theory*, 30(4), pp. 629-636.

Sampath, A., Shan, J., 2007. Building Boundary Tracing and Regularization from Airborne Lidar Point Clouds, *Photogrammetric Engineering & Remote Sensing*, 73(7), pp. 805-812.

Sohn, G. and Dowman, I., 2007. Data fusion of high-resolution satellite imagery and LiDAR data for automatic building extraction. *ISPRS Journal of Photogrammetry and Remote Sensing*, 62(1):43-63.

Sohn, G., Huang, X. and Tao. V., 2007. Using a binary space partitioning tree for reconstructing polyhedral building models from airborne LiDAR data. *Photogrammetric Engineering & Remote Sensing*. In print.

Weidner, U., Förstner, W., 1995. Towards Automatic Building Extraction from High Resolution Digital Elevation Models, *ISPRS Journal*, 50(4), pp. 38-49

Weidner, U., 1996. An Approach to Building Extraction from Digital Surface Models, in: *Proceedings of the 18th ISPRS Congress, Comm.Ⅲ, WG 2*, Vienna, Austria, pp. 924-929

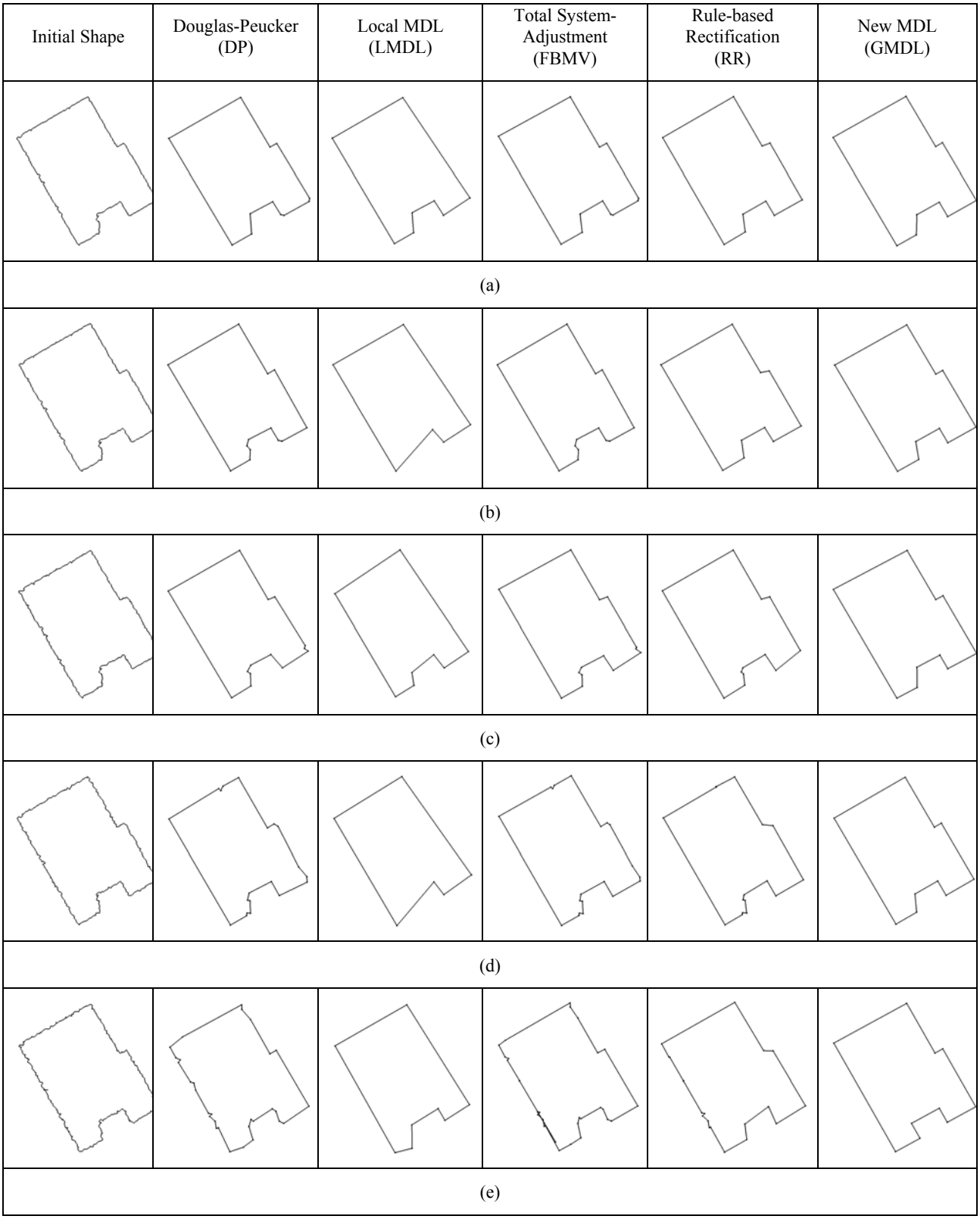

Figure 6. The results of regularization from initial boundary line with the random error of (a) ±5 cm, (b) ±10 cm, (c) ±15 cm, (d) ±20cm, and (e) ±25cm